MULTI-SCALE MODEL DRIVEN SINGLE IMAGE DEHAZING

Zhengguo Li and Haiyan Shu

SRO Department, Institute for Infocomm Research, 1 Fusionopolis Way, 138632 Singapore

ABSTRACT

Model driven single image dehazing was widely studied due to its broad applications. It is challenging to prevent noise from being amplified in sky region for the model driven dehazing algorithms. In this paper, a new multi-scale hazy image model is first built up by using the Laplacian pyramid of hazy image and the Gaussian pyramid of transmission map. A novel multi-scale dehazing algorithm is then proposed on top of the model to address the problem. Different haze removal and noise reduction approaches are applied to restore the scene radiance at different levels of the pyramid. The resultant pyramid is collapsed to restore a haze-free image. Experiment results demonstrate that the proposed algorithm outperform state of the art dehazing algorithms and the noise is indeed prevented from being amplified in the sky region.

1. INTRODUCTION

Under bad weather conditions such as haze, smoke, fog, and so on, an outdoor hazy image suffers from contrast loss of captured objects [1], reduction of depth and dynamic range [2, 3], as well as color distortion [4]. Single image dehazing is to restore a haze-free image from a single hazy image. The color distortion caused by the air-light is corrected as well as both the local and the global contrast of the scene are increased in the restored image [1]. The problem was well studied due to its broad applications including those in [5].

Existing single image dehazing algorithms can be classified into data driven algorithms and model driven algorithms. The data driven dehazing, especially deep learning based dehazing was quite popular. Ren et al. [6] and Cai et al. [7] proposed to study single image dehazing using deep convolutional neural networks (CNNs). All the CNN based algorithms have potential to obtain higher SSIM or PSNR values but the dehazed images look blurry and they are not photo realistic. Their performance also needs to be improved if the haze is heavy [8]. Qu et al. [9] proposed a generative adversarial nets (GANs) based dehazing algorithm, which generated a haze-free image without using the physical scattering model [10]. Unlike the CNN based algorithms, the GAN based dehazing algorithm is able to produce photo-realistic images even though generated texture is different from real one. However, the data driven algorithms perform poor on hazy images captured by cameras, especially for those hazy images with heavy haze [11].

An outdoor hazy image can be modelled by a pixel-wise convex combination of a haze-free image and a global atmospheric light [10]. Many model driven dehazing algorithms were proposed by using the model. Since the number of freedoms is larger than the number of observations, single image dehazing is an underconstrained problem. *Ambiguity between object radiance and haze* is one inherent problem for the model based singe image dehazing algorithms. Different priors were proposed to address the inherent problem. He et al. [4] introduced a well known dark channel prior (DCP) for single image dehazing. The DCP assumes that each local patch of an outdoor haze-free image includes at least one pixel which has at least one color channel with a small intensity. The patch is usually selected as 15×15 by the existing algorithms. The DCP introduces morphological artifacts to the restored image. Guided image filters (GIFs) [12] and weighted GIF (WGIF) [13] can be selected to smooth the morphological artifacts. The radius of the filter is usually chosen as 60 such that the morphological artifacts can be smoothed. On the other hand, fine structure cannot be preserved well by the GIF or WGIF with the large radius [14]. Even though the global GIF in [14] can be adopted to address this problem, its complexity is an issue for devices with limited computational resource. A haze line prior (HLP) was proposed in [15] to address the inherent problem. The HLP is based on an observation that the colors of a haze-free image can usually be represented by a finite number of different colors which are classified into clusters in the RGB space [16]. All pixels in each cluster form a haze line in the hazy image. The HLP assumes that each haze line includes at least one haze-free pixel. The algorithms in [4, 15] are robust to different degree of haze in hazy images.

The transmission map is very small for each pixel in sky region due to its large depth. Noise is amplified in the sky region of the dehazed image if the hazy image is noisy. This implies that *noise amplification in the sky region* is the other inherent problem for the Koschmiedars law based single dehazing algorithms. Li et al [13, 17] introduced an adaptive sky compensation term to address the problem. However, a pixel in the brightest object could be classified as a pixel in the sky region. Subsequently, haze of the brightest objects might not be removed well. It is thus desired to develop a new single image dehazing algorithm to address both the inherent problems and the algorithm is applicable regardless of haze degree.

In this paper, a novel multi-scale model driven dehazing algorithm is proposed to address all the above problems by using the Koschmiedars law [10] and the Laplacian pyramids [18]. Same as the DCP based dehazing algorithms [4, 17], the transmission map is assumed to be constant in a small neighborhood of each pixel. A new multi-scale hazy image model is first built up. The hazy and haze-free images are decomposed into multiple scales via the Laplacian pyramids which are on top of Gaussian pyramids. The transmission map is decomposed into multiple scales by using the Gaussian pyramid. It is found that *the relationship between the Gaussian pyramids of the hazy and haze-free images follows the Koschmiedars law at the different level*. The relationship between their Laplacian pyramids at the different level is derived from the Koschmiedars law and the new finding. A simple multi-scale dehazing algorithm is then proposed on top of the new model. The global atmospheric light is estimated by using the hierarchical searching method in [21], and the transmission map is estimated by using the HLP in [15]. Since the Laplacian pyramid of the hazy image contains different amount of noise at different level, different noise reduction method is adopted to recover the scene radiance at the different level of the pyramid. The resultant pyramid is finally collapsed to restore a dehazed image. Experimental results show that the proposed algorithm outperforms existing dehazing algorithms from both subjective quality and objective quality (such as dehazing quality index (DHQI) in [23]) points of view, and it can prevent noise from being amplified in the sky region regardless of haze degree.

The rest of this paper is organized as below. Inherent problems of model driven single image dehazing are presented in Section 2. A new multi-scale dehazing algorithm is proposed in Section 3. Experimental results are provided in Section 4 to verify the proposed algorithm. Conclusion remarks are drawn in Section 5.

2. INHERENT PROBLEMS OF MODEL DRIVEN SINGLE IMAGE DEHAZING

The relationship between a hazy image Z and a haze-free image I can be represented by the following Koschmiedars law [10]:

$$Z_c(i,j) = I_c(i,j)t(i,j) + A_c(1 - t(i,j)), \tag{1}$$

where (i,j) is a pixel position, and $c \in \{R, G, B\}$ is a color channel. A_c is the atmospheric light and is a constant for the whole image. t is the transmission map which describes the portion of the light reaching the camera. The term $I_c(i,j)t(i,j)$ is called direct attenuation, and the term $A_c(1 - t(i,j))$ is called airlight. When the atmosphere is homogenous, $t(i,j)$ can be computed by

$$t(i,j) = \exp^{-\alpha d(i,j)}, \tag{2}$$

and $\alpha(> 0)$ represents the scattering coefficient of the atmosphere. $d(i,j)$ is the depth of pixel (i,j).

Both the atmospheric light A and the transmission map t are estimated to restore a haze-free image. Consider a pixel (i,j) in the sky region, the transmission map $t(i,j)$ is almost zero and the value of $Z_c(i,j)$ is A_c. Thus, variance of pixel values is small and average of pixel values is large in the sky region. The atmospheric light A_c is usually larger than the $I_c(i,j)$. A hierarchical searching method was proposed in [21] to estimate the atmospheric light A by using these observations.

It is challenging to estimate the transmission map $t(i,j)$ for each pixel. The *ambiguity between object radiance and haze* is one inherent problem for the model driven singe image dehazing because there are only three equations but at least four unknown variable per pixel position. The challenging problem can be resolved by introducing different priors. The HLP in [15] is adopted in this paper because it can preserve fine structure better than the DCP. Define a set $H(i,j)$ as

$$H(i,j) = \{(i',j') | \sum_{c \in \{R,G,B\}} |I_c(i',j') - I_c(i,j)| = 0\}. \tag{3}$$

All the $Z(i',j')$'s with (i',j') in the set $H(i,j)$ form a haze line with the color $I(i,j)$ and the atmospheric light A as the two end points [15]. Each haze line can be identified by using a color shift hazy pixel $\hat{Z}(i',j')$ which is defined as $(Z(i',j') - A)$. The $\hat{Z}(i',j')$ can be converted into the spherical coordinates as $[r(i',j'),$ $\theta(i',j'),$ $\psi(i',j')]$. $\theta(i',j')$ and $\psi(i',j')$ are the longitude and latitude, respectively, and $r(i',j')$ is

$$r(i',j') = \|\hat{Z}(i',j')\| = t(i',j')\|I(i',j') - A\|. \tag{4}$$

Consider two pixel positions (i'_1, j'_1) and (i'_2, j'_2) in the set $H(i,j)$, it can be verified that

$$\theta(i'_1, j'_1) = \theta(i'_2, j'_2), \psi(i'_1, j'_1) = \psi(i'_2, j'_2). \tag{5}$$

In other words, all pixels are clustered into different haze lines according to $[\theta(i',j'), \psi(i',j')]$. The pixels in one cluster are usually located at different distances from the camera. Let $r_{max}(i,j)$ be defined as

$$r_{max}(i,j) = \max_{(i',j') \in H(i,j)} \{r(i',j')\}. \tag{6}$$

It was shown in [16] that the colors of a haze-free image can usually be represented by several hundred different colors. Thus, all the $Z(i',j')$'s form several hundred haze lines. The HLP in [15] assumes that each haze-line includes a haze-free pixel. In other words, $r_{max}(i,j)$ is $\|I(i,j) - A\|$. With the HLP, the $t(i,j)$ can be estimated as

$$t(i,j) = \frac{r(i,j)}{r_{max}(i,j)} \tag{7}$$

for each pixel position (i,j).

Once the atmospheric light A and the transmission map t are available, the haze-free image I can be recovered by:

$$I(i,j) = \frac{Z(i,j) - A}{\max\{t(i,j), t_0\}} + A, \tag{8}$$

where t_0 is a small constant such as 0.1 in [4].

Most existing haze removal algorithms assume that the hazy image Z is noise free. However, an outdoor hazy image Z is usually noisy [13, 8], and it can be represented by

$$Z(i,j) = \tilde{Z}(i,j) + n(i,j), \tag{9}$$

where $\tilde{Z}$ is a hazy but noise free image and n is the noise image. Combining the equations (8) and (9), the haze-free image is restored by

$$I(i,j) = \frac{\tilde{Z}(i,j) - A}{\max\{t(i,j), t_0\}} + A + \frac{n(i,j)}{\max\{t(i,j), t_0\}}. \tag{10}$$

Considering a pixel position (i,j) in the sky region, $d(i,j)$ is very large, and $t(i,j)$ is almost zero. Subsequently, $\max\{t(i,j), t_0\}$ is equal to t_0. The noise is amplified as $\frac{n(i,j)}{t_0}$, as shown in Eq. (10). This implies that *noise amplification in the sky region* is the other inherent problem for the model driven single image dehazing. Actually, the atmospheric light A and the transmission map t could also be affected by the noise if they are estimated from the noisy hazy image Z. A new multi-scale dehazing algorithm will be proposed to address the problems in the next section.

3. MULTI-SCALE DEHAZING

In this section, a multi-scale hazy image model is first built up by using the Koschmiedars law (1) and the Laplacian pyramid [18, 19, 20]. A novel multi-scale dehazing algorithm is then proposed. Finally, the proposed algorithm is analyzed.

3.1. A Laplacian Pyramid Hazy Image Model

A Laplacian pyramid is usually generated on top of a Gaussian pyramid [18]. Let $\{Z\}_G^l$ be the $l(0 \le l \le L_0)$-th level in the Gaussian pyramid of the image Z. L_0 is chosen as 2 in this paper. The pyramid is generated as [18]

$$\{Z\}_G^l = \Psi(\{Z\}_G^{l-1}) \tag{11}$$

where $\{Z\}_G^0$ is Z, $l = 1, \cdots, L_0$, and $\Psi(\cdot)$ is defined as

$$\left\{\begin{array}{l} \{Z\}_G^l(i,j) = \sum_{m=-1}^{1}\sum_{n=-1}^{1} w(m,n)\{Z\}_G^{l-1}(2i+m, 2j+n) \\ w(m,n) = \tilde{w}(m)\tilde{w}(n) \\ \tilde{w}(-1) = \tilde{w}(1) = \frac{1}{4}\ ;\ \tilde{w}(0) = \frac{1}{2} \end{array}\right. . \tag{12}$$

Let $\{Z\}_L^l$ be the Laplacian pyramid of the image Z and it is generated by [18]

$$\left\{\begin{array}{l} \{Z\}_L^{l-1} = \{Z\}_G^{l-1} - \{Z\}_E^{l-1} \\ \{Z\}_E^{l-1} = \Phi(\{Z\}_G^l) \end{array}\right. , \tag{13}$$

where $\Phi(\cdot)$ is the reverse of $\Psi(\cdot)$ and it is defined as [18]

$$\{Z\}_E^{l-1}(i,j) = 4\sum_{m=-1}^{1}\sum_{n=-1}^{1} w(m,n)\{Z\}_G^l(\frac{i-m}{2}, \frac{j-n}{2}), \tag{14}$$

and only terms for which $(i-m)/2$ and $(j-n)/2$ are integers are included in the sum.

The Gaussian pyramid of the transmission map t is denoted as $\{t\}_G^l$. Similar to the existing dehazing algorithms [4, 17], the transmission map t is assumed to be constant in a small neighborhood of each pixel. It can be easily shown that

$$\{t\}_G^l(i,j) = \{t\}_G^{l-1}(2i+m, 2j+n) = \{t\}_E^{l-1}(2i, 2j) \tag{15}$$

hold for all $l(0 \le l \le L_0)$'s and $m, n \in \{-1, 0, 1\}$ if L_0 is small.

For simplicity, the hazy image Z is first assumed to be noise free. It can be derived from the equations (1), (11), (12) and (15) that

$$\begin{aligned} \{Z\}_G^1(i,j) &= \{I\}_G^1(i,j)t(2i,2j) + A(1 - t(2i,2j)) \\ &= \{I\}_G^1(i,j)\{t\}_G^1(i,j) + A(1 - \{t\}_G^1(i,j)), \end{aligned} \tag{16}$$

and from the equations (13), (15) and (16) that

$$\begin{aligned} \{Z\}_L^0(i,j) &= Z(i,j) - \{Z\}_E^0(i,j) \\ &= (I(i,j) - \{I\}_E^0(i,j))t(i,j) \\ &= \{I\}_L^0(i,j)t(i,j) \\ &= \{I\}_L^0(i,j)\{t\}_G^0(i,j). \end{aligned} \tag{17}$$

Similarly, it can be derived that

$$\left\{\begin{array}{l} \{Z\}_G^l(i,j) = (\{I\}_G^l(i,j) - A)\{t\}_G^l(i,j) + A \\ \{Z\}_L^l(i,j) = \{I\}_L^l(i,j)\{t\}_G^l(i,j) \end{array}\right. \tag{18}$$

holds for all $l(0 \le l \le L_0)$'s. Clearly, the relationship between the Gaussian pyramids of the hazy and haze-free images also follows the Koschmiedars law at the different level. The Laplacian components of the hazy image are scaled down. As a result, the contrast of the hazy image is reduced.

Similar results can be derived for a noisy and hazy image Z. The proposed multi-scale hazy image model is finally presented as

$$\left\{\begin{array}{l} \{Z\}_G^{L_0}(i,j) = (\{I\}_G^{L_0}(i,j) - A)\{t\}_G^{L_0}(i,j) + A \\ \{Z\}_L^l(i,j) = \{I\}_L^l(i,j)\{t\}_G^l(i,j) + \{n\}_L^l(i,j) \end{array}\right. , \tag{19}$$

where $0 \le l < L_0$. This model is based on the facto that $\{Z\}_G^{L_0}$ is usually noise free. It can be easily verified that $\{Z\}_L^{l-1}$ includes much more noise than $\{Z\}_L^l$, i.e., $\{n\}_L^l(i,j) \ll \{n\}_L^{l-1}(i,j)$.

3.2. The Proposed Algorithm

Since the image $\{Z\}_E^0$ includes less noise than the hazy image Z, both the atmospheric light A and the transmission map t are estimated by using $\{Z\}_E^0$ rather than the hazy image Z as in [4, 15, 17]. The atmospheric light A is estimated by using the hierarchical searching method on basis of the quad-tree subdivision in [21], and the transmission map $t(i,j)$ is estimated via the HLP in [15].

Since the Laplacian pyramid of the hazy image contains different amount of noise at the different level, different noise reduction method is proposed to recover the scene radiance at the different level of the pyramid. At the coarsest level L_0, the Gaussian component of the scene radiance is restored as

$$\{I\}_G^{L_0}(i,j) = \frac{\{Z\}_G^{L_0}(i,j) - A}{\max\{\{t\}_G^{L_0}(i,j), \eta)} + A, \tag{20}$$

where η is 1/4 for normal haze and 1/8 for heavy haze.

At the level $l(0 \le l < L_0)$, the Laplacian component of the scene radiance is recovered by

$$\begin{aligned} \{I\}_L^l(i,j) =& (1 - \frac{\phi(\{t\}_G^l(i,j))}{2^l})\frac{\{Z\}_L^l(i,j)}{\max\{\{t\}_G^l(i,j), \eta\}} \\ &+ \frac{\phi(\{t\}_G^l(i,j))}{2^l}\psi(\{t\}_G^l(i,j))\{Z\}_L^l(i,j), \end{aligned} \tag{21}$$

where functions $\phi(\cdot)$ and function $\psi(\cdot)$ are defined as

$$\left\{\begin{array}{l} \phi(\{t\}_G^l(i,j)) = \frac{1}{1+\exp(32(\frac{\{t\}_G^l(i,j)}{\eta} - 1))} \\ \psi(\{t\}_G^l(i,j)) = \frac{\{t\}_G^l(i,j)}{\eta} + 1 \end{array}\right. . \tag{22}$$

Two important cases of the equation (21) are addressed as follows:

Case 1: $\{t\}_G^l(i,j)$ is less than η, $\phi(\{t\}_G^l(i,j))$ is almost 1. It can be derived from the equation (21) that

$$\{I\}_L^l(i,j) \approx (1 - \frac{1}{2^l})\frac{\{Z\}_L^l(i,j)}{\eta} + \frac{1}{2^l}\psi(\{t\}_G^l(i,j))\{Z\}_L^l(i,j).$$

Considering the cases that $l = 0$, $l = 1$ and $\{t\}_G^l(i,j) \approx 0$, it can be derived that

$$\left\{\begin{array}{l} \{I\}_L^1(i,j) \approx \frac{1}{2}\frac{\{Z\}_L^l(i,j)}{\eta} + \frac{1}{2}\{Z\}_L^l(i,j) \\ \{I\}_L^0(i,j) \approx \{Z\}_L^1(i,j) \end{array}\right. .$$

Since the noise is reduced from the finest level to the coarsest level, the weight of $\frac{\{Z\}_L^l(i,j)}{\eta}$ is decreased from the coarsest level to the finest level. Clearly, the noise is prevented from being amplified in the sky region by using the proposed multi-scale single

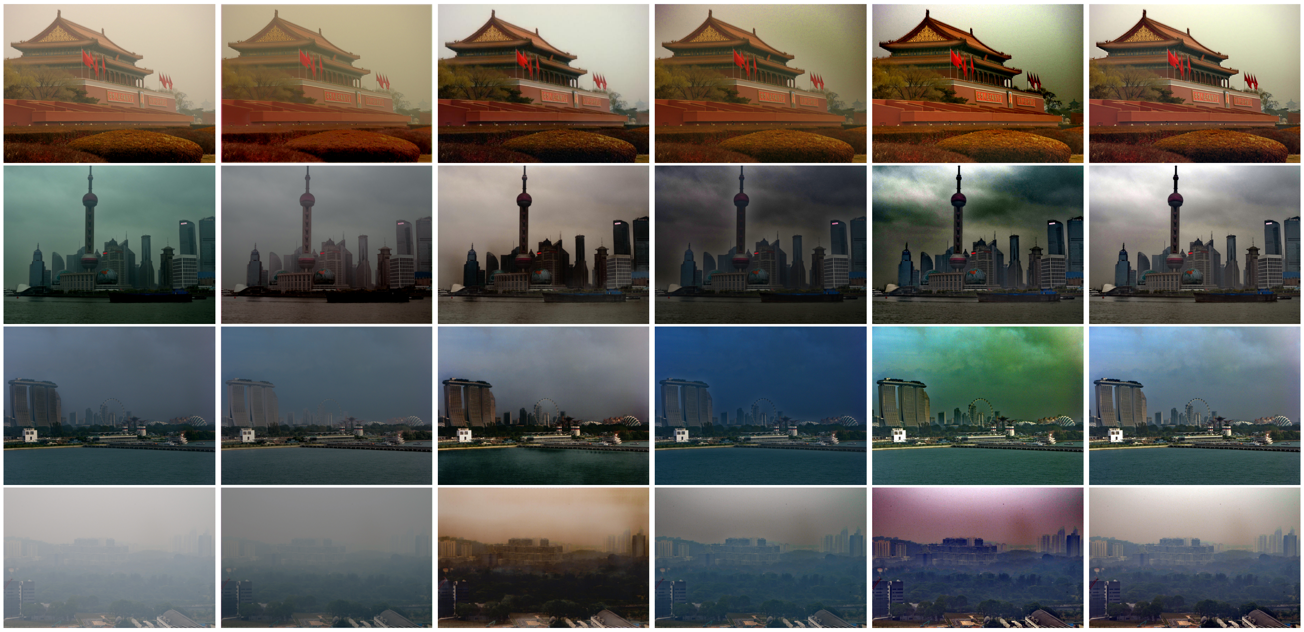

Fig. 1. Comparison of different haze removal algorithms. From left to right, dehazed images by the algorithms proposed by [7], [22], [9], [4], [15] and ours, respectively.

image dehazing algorithm.

Case 2: $\{t\}_G^l(i,j)$ is larger than η, $\phi(\{t\}_G^l(i,j))$ is almost 0. It can be derived from the equation (21) that

$$\{I\}_L^l(i,j) \approx \frac{\{Z\}_L^l(i,j)}{\{t\}_G^l(i,j)}.$$

Subsequently, objects nearby the camera are restored well. It is shown in these two cases that single image dehazing is indeed one type of spatially varying single image detail enhancement [13].

The pyramid of $\{I\}_G^{L_0}$ and $\{I\}_L^l(0 \leq l < L_0)$ is collapsed to obtain the haze-free image I. All the Laplacian components $\{I\}_L^l(i,j)$'s can be tuned according to users' preference. For example, they can be amplified to produce a sharper haze-free image.

4. EXPERIMENTAL RESULTS

Experimental results are provided in this section to demonstrate the proposed multi-scale dehazing algorithm. Readers are invited to view to electronic version of figures and zoom in them so as to better check differences among all images.

The proposed algorithm is compared with five state-of-the-art dehazing algorithms in [4], [15], [7], [9], and [22] by testing 21 real outdoor hazy images [24]. It should be pointed out that the algorithms in [4] and [15] are model driven algorithms while the others are data driven algorithms. As shown in Fig. 1, the dehazed images by the algorithms in [7] and [22] are too blurry and they are not photo-realistic. The haze is not removed well if it is heavy. The algorithm in [9] can be applied to overcome the problems but the generated texture is different from real one. Color distortion is also a possible issue for all the learning based dehazing algorithms. Therefore, the deep learning based dehazing algorithms could not perform well for real hazy images. The model driven algorithms in [4], [15] and the proposed algorithm can be applied to generate photo realistic images with the real texture. Both the algorithm in [15] and the proposed algorithm preserve fine structures than the algorithm in [4]. Noise is indeed amplified in the sky regions of the dehazed images by the model driven algorithms [4] and [15]. The problem is overcome by the proposed multi-scale dehazing algorithm due to the equation (21). Overall, the proposed algorithm outperforms other algorithms from the subjective quality point of view.

Besides the subjective evaluation, the quality index DHQI in [23] is adopted to compare the proposed algorithm with the algorithms in [4], [15], [7], [9], and [22]. Each dehazed images of [9] is upsampled to be consistent with the size of the input. The average DHQI values of the 21 outdoor hazy images are given in Table 1. Clearly, the proposed algorithm also outperforms other algorithms from the objective quality point of view.

Table 1. Average DHQI values of 21 real outdoor hazy images for different algorithms (the larger, the better).

[4]	[15]	[7]	[9]	[22]	Ours
50.55	51.96	53.09	46.67	45.52	**56.45**

5. CONCLUSION

In this paper, a new multi-scale hazy image model has been built up by using the Laplacian pyramid of the hazy image, the Gaussian pyramid of the transmission map and the Koschmiedars law. A novel multi-scale algorithm has then been introduced using the new model. Experiment results validate the proposed algorithm.

It is worth noting that both the Gaussian and Laplacian pyramids are on top of linear filters which cannot preserve edges well. Subsequently, there are aliasing artifacts around edge which are amplified in single image dehazing. This problem can be addressed by using an edge-preserving filter [25] and it will be studied in our future research.

References

[1] S. G. Narasimhan and S. K. Nayar, “Contrast restoration of weather degraded images,” IEEE Trans. Pattern Anal. Mach. Learn., vol. 25, no. 6, pp. 713-724, Jun. 2003.

[2] P. E. Debevec and J. Malik, “Recovering high dynamic range radiance maps from photographs”, in *Proc. of the 1997 Conference on Computer Graphics (SIGGRAPH)*, pp. 369-378, 1997.

[3] J. H. Zheng, Z. G. Li, Z. J. Zhu, S. Q. Wu, and S. Rahardja, “Hybrid patching for a sequence of differently exposed images with moving objects,” IEEE Trans. on Image Processing, vol. 22, no. 12, pp.5190-5201, Dec. 2013.

[4] K. He, J. Sun, and X. Tang, “Single image haze removal using dark channel prior,” IEEE Trans. On Pattern Analysis and Machine Learning, vol. 33, no. 12, pp. 2341-2353, Dec. 2011.

[5] G. Li, C. Wen, Z. Li, F. Yang, and K. Mao, “Model based online learning with kernels,” IEEE Trans. on Neural Networks and Learning Systems, vol. 24, no. 3, 356-369, Mar. 2013.

[6] W. Ren, S. Liu, H. Zhang, J. Pan, and X. Cao, “Single image dehazing via multi-scale convolutional neural networks”, in *Proceedings of the European Conference on Computer Vision*, pp 154-169, Sept. 2016.

[7] B. Cai, X. Xu, K. Jia, C. Qing, and D. Tao, “Dehazenet: an end-to-end system for single image haze removal,” IEEE Trans. on Image Processing, vol. 25, no. 11, pp. 5187-5198, Nov. 2016.

[8] A. Golts, D. Freedman, and M. Elad, “Unsupervised single image dehazing using dark channel prior loss,” IEEE Trans. on Image Processing, vol. 29, pp. 2692 - 2701, Nov. 2019.

[9] Y. Qu, Y. Chen, J. Huang, and Y. Xie, “Enhanced Pix2pix dehazing network,” In *Proceedings of the IEEE Conference on Computer Vision and Pattern Recognition*, pp. 8152-8160, Jun. 2019.

[10] H. Koschmider, “Theorie der horizontalen sichtweite,” in *Proc. Beitrage Phys. Freien Atmos.*, pp. 33-53, 1924.

[11] W. Liu, F. Zhou, J. Duan, and G. Qiu, “Image defogging quality assessment: real-world database and method,” IEEE Trans. on Image Processing, vol. 30, pp. 1762-190, Mar. 2021.

[12] K. He, J. Sun, and X. Tang, “Guided image filtering,” IEEE Trans. on Pattern Analyis and Machine Intelligence, vol. 35, no. 6, pp. 1397-1409, Jun. 2013.

[13] Z. G. Li, J. H. Zheng, Z. J. Zhu, Y. Wei, and S. Q. Wu, “Weighted guided image filtering,” IEEE Trans. on Image Processing, vol. 24, no. 1, pp.120-129, Jan. 2015.

[14] Z. G. Li and J. H. Zheng, “Single image haze removal using globally guided image filtering,” IEEE Trans. on Image Processing, vol. 27, no. 1, pp. 442-450, Jan. 2018.

[15] D. Berman, T. Treibitz, and S. Avidan, “Non-local image dehazing,” in *Proceedings of the IEEE Conference on Computer Vision and Pattern Recognition*, pp. 1674-1682, 2016.

[16] M. T. Orchard and C. A. Bouman, “Color quantization of images,” IEEE Trans. on Signal Processing, vol. 39, no. 12, pp. 2677–2690, Dec. 1991.

[17] Z. G. Li and J. H. Zheng, “Edge-preserving decomposition-based single image haze removal,” IEEE Trans. on Image Processing, vol. 24, no.12, 5432-5441, Dec. 2015.

[18] P. J. Burt and E. H. Adelson, “The Laplacian pyramid as a compact image code,” IEEE Trans. Communication, vol. 31, no. 4, pp. 532-540, Apr. 1983.

[19] C. O. Ancuti and C. Ancuti, “Single image dehazing by multi-scale fusion,” IEEE Trans. Image Process., vol. 22, no. 8, pp. 3271–3282, Aug. 2013.

[20] F. Kou, Z. Li, W. Chen, and C. Wen, “Multi-scale exposure fusion via gradient domain guided image filtering,” in *IEEE 2017 International Conference on Multimedia and Expo*, Hongkong, Jul. 10-14, 2017.

[21] J. H. Kim, W. D. Jang, J. Y. Sim, and C. S. Kim, “Optimized contrast enhancement for real-time image and video dehazing,” Journal of Visual Communication and Image Representation, vol. 24, no. 3, pp. 410-425, Apr. 2013.

[22] B. Li, X. Peng, Z. Wang, J. Xu, and D. Feng, “AOD-Net: all-in-one dehazing network,” in *Proceedings of the IEEE International Conference on Computer Vision*, pp. 4780-4788, Oct. 2017.

[23] X. Min, G. Zhai, K. Gu, X. Yang, and X. Guan, “Objective quality evaluation of dehazed images,” IEEE Trans. on Intelligent Transportation Systems, vol. 20, no. 8, pp. 2879-2892, Aug. 2019.

[24] https://github.com/zhengchaobing/Dehazing.

[25] F. Kou, W. Chen, C. Wen, and Z. Li, “Gradient domain guided image filtering,” IEEE Trans. on Image Processing, vol. 24, no. 11, pp.4528-4539, Nov. 2015.